Annals of Nuclear Medicine Vol. 19, No. 2, 83–89, 2005

Accuracy of cardiac PET imaging using post-injection transmission scan

Tatsuya YONEYAMA,*,** Ichiro MATSUNARI,** Sugako KANAYAMA,*** Masamichi MATSUDAIRA,** Kenichi NAKAJIMA,* Junichi TAKI,* Stephan G. NEKOLLA,**** Kinichi HISADA** and Norihisa TONAMI*

*Department of Biotracer Medicine, Kanazawa University School of Medicine, Kanazawa, Japan
**The Medical and Pharmacological Research Center Foundation, Ishikawa, Japan
***Department of Cardiology, Kanazawa Medical University, Ishikawa, Japan
****Nukleamedizinische Klinik und Poliklinik Technische Universitat Munchen, Munich, Germany

The purpose of this study was to investigate the accuracy of cardiac PET with post-injection transmission scans. ***Methods:*** We performed a phantom study using ^{18}F solution as well as ^{13}N-ammonia PET study of ten patients. The average activities of no myocardial defect phantom model were estimated, and myocardial defect sizes of 12 phantom models were measured by pre- and post-injection transmission methods at various ^{18}F activities. In ^{13}N-ammonia PET at rest and during adenosine triphosphate (ATP) stress studies, measured defect sizes were compared between both methods. ***Results:*** The ratios of average activity estimated by both methods (post/pre value) were almost 1.00 at each ^{18}F activity and segment. Measured defect sizes by both methods showed an excellent correlation with true defect sizes ($r = 0.98$, $p < 0.01$ for pre vs. true value: $r = 0.98$, $p < 0.01$ for post vs. true value). The mean absolute errors of measurements were minimal up to 3.5% LV, and were similar between both methods. In ^{13}N-ammonia PET, measured defect sizes by both methods also showed a good correlation ($r = 0.97$, $p < 0.01$). ***Conclusion:*** The results indicate that cardiac PET imaging with post-injection transmission scan provides information on myocardial tracer activity as well as myocardial defect size as does conventional pre-injection transmission method.

Key words: post-injection transmission, PET, cardiac phantom, patients with coronary artery disease, ATP

INTRODUCTION

CARDIAC PET IMAGING is considered as a reliable technique to assess myocardial blood flow and viability.[1–3] In conventional PET acquisition, transmission scan is performed before tracer injection, which is followed by subsequent emission scan, referred to here as pre-injection transmission scan. Thus, patients are required to remain motionless from the start of the transmission scan to the end of the emission scan. A potential problem of this procedure is that patients may move on a scanner bed because it is uncomfortable to lie on the scanner bed for a long period. A perfect match between transmission and emission data is required in order to perform an accurate attenuation correction, which is important to perform quantitative PET measurements.[4] An alternative approach, in which transmission scan is performed after emission scan, referred to here as post-injection transmission scan,[5,6] would significantly reduce the study duration for patients, resulting in increased patient comfort and throughput, and improved patient translation on a scanner bed. However, the accuracy of PET measurements using post-injection transmission scan has not been extensively investigated for cardiac studies. Post-injection transmission data could cause errors because of increased noise in transmission data caused by the subsequent subtraction of extra emission counts.

The purpose of this study was to investigate whether cardiac PET imaging with post-injection transmission scan provides quantitative information on myocardial

Received July 5, 2004, revision accepted October 27, 2004.
For reprint contact: Tatsuya Yoneyama, M.D., The Medical and Pharmacological Research Center Foundation, Wo 32, Inoyama, Hakui, Ishikawa 925–0613, JAPAN.
E-mail: yoneyama@nmd.m.kanazawa-u.ac.jp

radiotracer activity and defect size as accurate as conventional pre-injection transmission method.

MATERIALS AND METHODS

Cardiac phantom

All acquisitions of phantom study were performed using an elliptical cylinder chest phantom with simulated bone, lung, mediastinum, liver, and a cardiac phantom (Model HL, Anzai Co. Ltd., Tokyo, Japan). The characteristics of the phantom were described elsewhere.[7] In brief, the size of chest phantom is 320 mm width by 220 mm depth by 210 mm height. The phantom consists of a right ventricle and left ventricle with separate compartments for the blood pool and the myocardium. Fluorine-18 solution, to simulate clinical studies employing ^{18}F-FDG, was given into the left ventricular (LV) myocardium (400 kBq/m*l*), mediastinum (40 kBq/m*l*), right and left ventricular cavities (40 kBq/m*l*), and liver (160 kBq/m*l*). Plastic inserts, ranging in size from 2–60% of the myocardium (n = 12), were used to simulate transmural myocardial scars. We examined 6 anterior and 6 inferior defect models. One model with no defect was also examined as a normal model.

Patients with coronary artery disease

Ten patients (9 men, 1 woman; age range 32–85 yr; mean age 58 ± 16 yr) with coronary artery disease based on age, sex, history and exercise electrocardiogram were studied. Of these patients, 3 had myocardial infarction. All subjects signed an informed consent form based on the guidelines of the institutional human study committee prior to participation in the study.

PET scanner

PET imaging was performed using a full-ring PET scanner (Advance, General Electric Medical Systems, Milwaukee, WI) with an in-plane spatial resolution of 3.8 mm FWHM at the exact center (the "sweet spot") of the field of view, and axial resolution of 4 mm.[8]

Phantom study

The imaging procedure of a phantom study is outlined in Figure 1. This procedure was performed in twelve cardiac phantom models with myocardial defect and one normal model with no defect.

After positioning the chest phantom on the scanner bed, static emission data were acquired for 640 seconds, and then transmission data were acquired for 640 seconds using two rotating Ge-68 pin sources.[9] The radioactivity of each Ge-68 pin source was 400 MBq. Subsequently, the acquisition procedure was repeated at 1, 2, 3, 4 physical half-lives of ^{18}F in the phantom in order to change ^{18}F activity in LV myocardium (400 kBq/m*l*, 200 kBq/m*l*, 100 kBq/m*l*, 50 kBq/m*l*, 25 kBq/m*l*). The phantom was kept at the same position in the gantry until the transmission scan was completed on the following day, acquired for 640 seconds, allowing for the physical decay of ^{18}F activity in the phantom. All acquisitions were operated in two dimensional (2-D) mode.

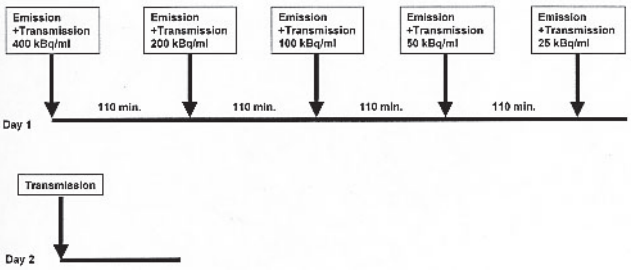

Fig. 1 Schematic representation of a phantom study imaging protocol.

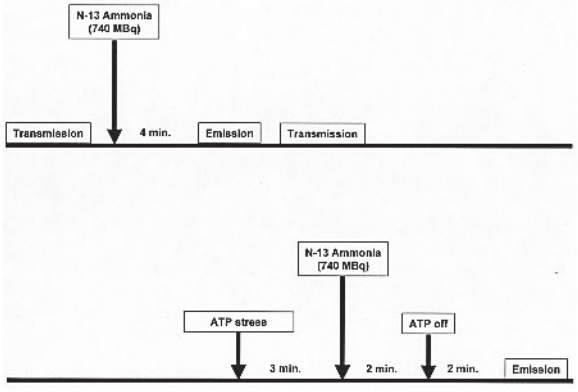

Fig. 2 Schematic representation of a clinical study imaging protocol.

Clinical study

^{13}N-ammonia PET studies of ten patients at rest and during ATP stress studies were performed. The imaging procedure of a clinical study is outlined in Figure 2. After positioning the patient on the scanner bed, transmission data were acquired for 15 min. Rest images were acquired for 5 min beginning 4 min after an intravenous injection of ^{13}N-ammonia (740 MBq). Subsequently, post-injection transmission data were acquired for 15 min. After the physical decay of ^{13}N-ammonia, ATP was infused intravenously at 0.16 mg/kg/min for 5 minutes. ^{13}N-ammonia was injected at 3 min during ATP infusion. ATP stress images were acquired, as above, for 5 min beginning 4 min after administration of ^{13}N-ammonia with the same dose of the rest study. All acquisitions of clinical study were also operated in 2-D mode.

Reconstruction

Images were reconstructed using a standard filtered backprojection algorithm with a Hann filter with cutoff frequency of 0.54 cycle/cm and a zoom of 1.57. The image data matrix was 128 × 128 with pixel sizes of 2.73 mm and

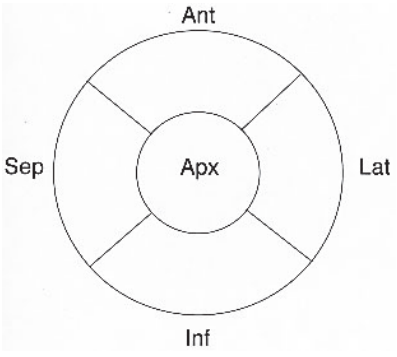

Fig. 3 Semiquantitative polar map analysis of cardiac phantom model with no defect. LV myocardium is divided into 5 regions (anterior, septal, inferior, lateral wall and apex).

Table 1 Ratio of myocardial ^{18}F-FDG activity (post/pre)

Activity (kBq/m*l*)	anterior	septum	inferior	lateral	apex
400	0.99	0.99	0.99	0.99	1.00
200	1.00	1.01	1.00	1.00	1.01
100	1.00	1.01	1.01	1.02	1.01
50	1.00	1.02	1.00	1.02	1.00
25	1.05	1.00	1.00	1.00	1.00

a slice thickness of 4.25 mm. Both attenuation and scatter corrections were employed during image reconstruction.

Correction for emission contamination

Transmission data in the presence of emission activity (T + E data), post-injection transmission data, were corrected for emission contamination using T + E subtraction.[10] The T + E subtraction is a method that estimates the emission contamination counts using emission scan which is either immediately preceding or following transmission scan, and then subtracts that estimate from the transmission data. In our study, the emission scan that followed the transmission scan was used for T + E subtraction.

Data analysis

All PET data were transferred to an Octane workstation (Silicon Graphics, Mountain View, CA) via ethernet, and were analyzed using a semiquantitative polar map approach,[11,12] which has been developed and validated at Munich Technical University. Briefly, an observer defined the long axis manually, and then the program automatically optimized sampling parameters using this axis as the initial estimate. The basal plane of the study was automatically determined, and a volumetric sampling algorithm encompressing the left ventricle with 540 sampling locations was used to generate polar maps.

In the phantom study, LV myocardium of no defect model was divided into anterior, inferior, septal, lateral and apical regions, as shown in Figure 3. The average activities of no defect model were calculated by pre- and post-injection transmission methods for each segment at 25, 50, 100, 200 and 400 kBq/m*l* of ^{18}F activities in LV myocardium, and were compared between both methods. Myocardial defect sizes were expressed as a percentage of total left ventricular myocardial mass (%LV), and compared to true defect sizes, which were directly measured from cardiac phantom models. The twelve defect model studies were used to obtain a correlation of true versus measured defect size by linear regression analysis for pre- and post-injection transmission methods. Estimated error (%LV-true defect size) and absolute error (absolute value of estimated error) were calculated for twelve defect models, and the mean absolute error (an average of absolute error of twelve defect models) was determined at each ^{18}F activity.[13]

Additionally, measured defect sizes by ^{13}N-ammonia PET of ten patients at rest and during ATP stress studies also were compared between both methods.

The cut-off threshold for the estimation of defect size was determined at 50% of peak activity, according to our prior study.[7]

Statistical analysis

Data were expressed as a mean ± 1 standard deviation (SD). Student's t-test was used to determine whether the mean estimated error was different from zero. Linear regression was performed by least-squares analysis. The Bland-Altman analysis of agreement was used to demonstrate the estimation errors in the measured defect size.[14] Statistical significance was defined as $p < 0.05$.

RESULTS

The ratio of the average activity estimated by pre- and post-injection transmission methods

Table 1 indicates the ratio of average activity of the no defect phantom model for each segment estimated by pre- and post-injection transmission methods at 25, 50, 100, 200 and 400 kBq/m*l* of ^{18}F activity in LV myocardium. As shown in Table 1, the ratios were almost 1.00 at each ^{18}F activity and myocardial segment, and the mean ratios of all segments were 1.01 ± 0.021 at 25 kBq/m*l*, 1.01 ± 0.013 at 50 kBq/m*l*, 1.01 ± 0.008 at 100 kBq/m*l*, 1.00 ± 0.003 at 200 kBq/m*l* and 0.99 ± 0.007 at 400 kBq/m*l*, respectively. Significant differences were not observed between ^{18}F activities in LV myocardium.

These results indicate that average activities estimated by post-injection transmission method were virtually identical to those by pre-injection transmission method within the range of tracer activity from 25 to 400 kBq/m*l* in LV myocardium.

Comparison of measured defect sizes by pre- and post-injection transmission methods

Figures 4A and 4B display the relationship between true

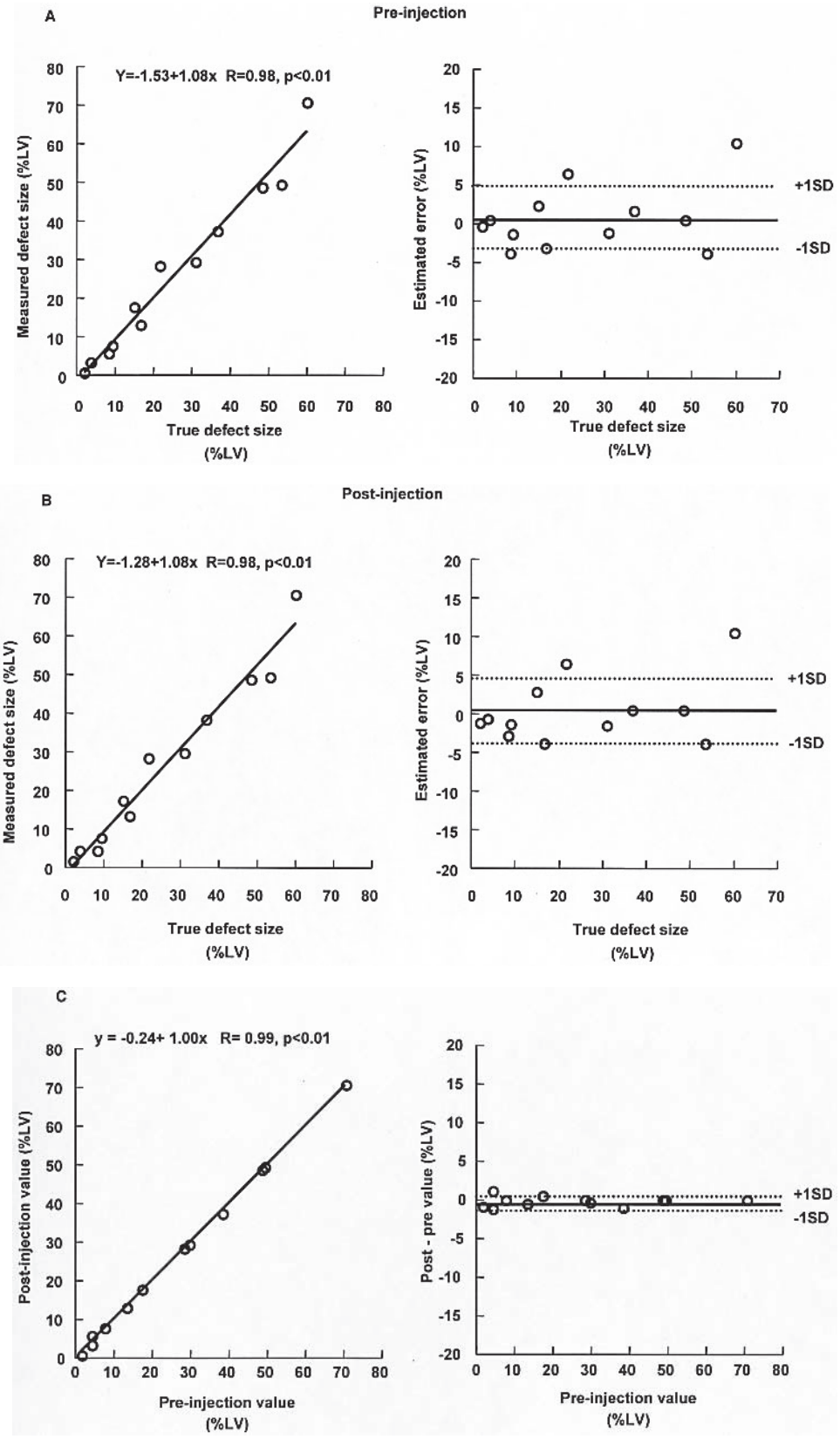

Fig. 4 Comparison of true defect size and measured defect size by pre-(A) or post-(B) injection transmission method when acquired at 400 kBq/m*l* in LV myocardium. Left graph represents plots of true defect size versus measured defect size, and right one represents the Bland-Altman analysis of agreement between true defect size and measured defect size. Similarly, comparison between both methods when acquired at 400 kBq/m*l* is represented in Figure 4C.

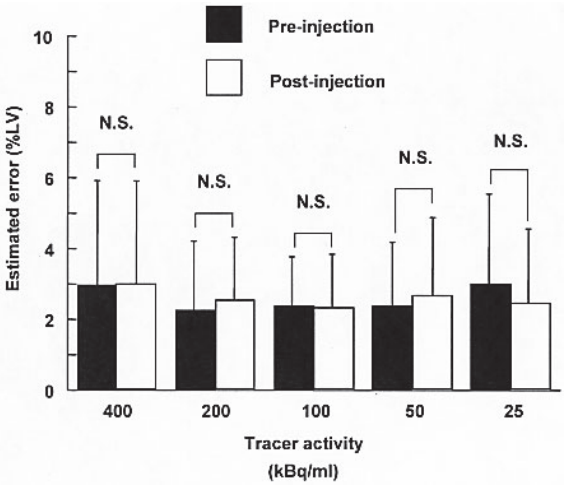

Fig. 5 Percentage error between true defect size and measured defect sizes by pre- or post-injection transmission methods at various ^{18}F activities.

defect sizes and measured defect sizes by pre- or post-injection transmission method, and Figure 4C displays the relationship between both methods when acquired at 400 kBq/m*l* of ^{18}F activity in LV myocardium. Measured defect sizes by both methods showed an excellent correlation with true defect sizes and with each other ($r = 0.98$: $p < 0.01$ for pre vs. true value, $r = 0.98$: $p < 0.01$ for post vs. true value, $r = 0.99$: $p < 0.01$ for pre vs. post value). The Bland-Altman plot of errors between true defect sizes and measured defect sizes by pre- and post-injection transmission methods and between pre- and post-injection transmission methods revealed that there was no systematic measurement bias.

Figure 5 displays the mean absolute error between true defect sizes and measured defect sizes by pre- or post-injection transmission method at various ^{18}F activities. The mean absolute errors of measurements were minimal up to 3.5% LV, and were similar between both methods at

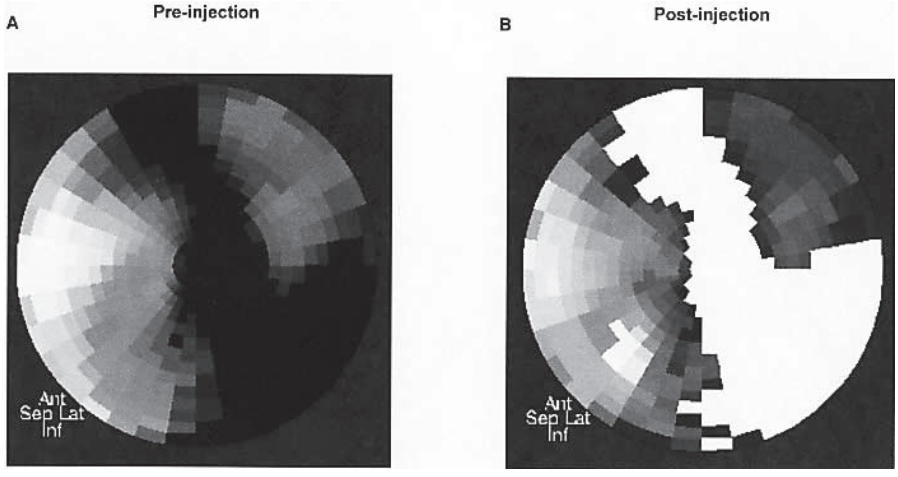

Fig. 6 The polar maps of ^{13}N-labeled ammonia PET during ATP stress images of a patient with coronary artery disease by pre-(A) and post-(B) injection transmission methods.

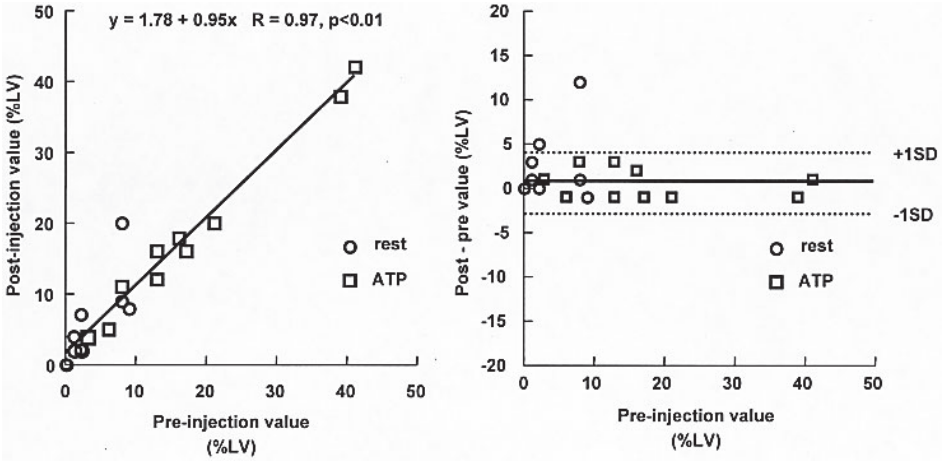

Fig. 7 Comparison of measured defect sizes by pre- and post-injection transmission methods of ^{13}N-ammonia PET of ten patients at rest and during ATP stress. Left graph represents plots of measured defect size by pre- versus post-injection transmission method, and right one represents the Bland-Altman analysis of agreement between both methods.

each ^{18}F activity. No statistical significance was seen in any phantom measurement between both methods.

Figure 6 displays the polar maps of ^{13}N-ammonia PET during ATP stress images of a patient with coronary artery disease. Myocardial defect areas were represented as black (A: pre-injection) and white (B: post-injection). By visual inspection, the image by post-injection transmission method provided useful information on myocardial defect area, such as its size and location, similar to that by pre-injection transmission method. Actually, the measured defect sizes by both methods were almost the same in this subject (pre value 41% LV, post value 42% LV).

Figure 7 displays the relationship between pre- and post-injection transmission methods of ^{13}N-ammonia PET of ten patients at rest and during ATP stress studies. Measured defect sizes by post-injection transmission method also showed an excellent correlation with those by pre-injection transmission method in clinical studies ($r = 0.97$, $p < 0.01$).

DISCUSSION

Although the accuracy of conventional PET measurement (pre-injection method) has been demonstrated by previous studies and accepted as a gold standard, PET measurement by post-injection transmission method has not been examined extensively in a quantitative manner for cardiac studies.

Our results were as follows: (a) the ratios of average activity estimated by pre- and post-injection transmission methods from no myocardial defect model were almost 1.00 within the range of tracer activity from 25 to 400 kBq/m*l* in LV myocardium, (b) measured defect sizes by both methods showed an excellent correlation with true defect sizes, and the mean absolute errors of measurements were minimal up to 3.5% LV and were similar between both methods at various ^{18}F activities, (c) measured defect sizes by post-injection transmission method of ^{13}N-ammonia PET of ten patients at rest and during ATP stress studies showed an excellent correlation with those by pre-injection transmission method.

One of the potential problems of post-injection transmission method is the statistical noise that is increased due to the subsequent subtraction of emission contamination from post-injection transmission data. The subtraction of a large amount of emission contamination would increase the noise in post-injection transmission data significantly. The increased noise may have a significant effect on post-injection transmission data, because attenuation correction could not be performed accurately if a noisy transmission data map was applied. Meanwhile, emission contamination would be reduced by using the limited injection dose. However, the image quality would get worse, and eventually quantitative PET measurements could not be achieved accurately. Thus, there would be an optimum range for tracer injection dose. In our phantom study, ^{18}F activities in LV myocardium ranged from 25 to 400 kBq/m*l* in order to change the amount of extra emission counts included in post-injection transmission data, and the results described as above indicate that, within the range of tracer activity in this study, the subtraction might be performed without increasing the noise significantly and that tracer activity in LV myocardium also was not significantly low enough to reduce the accuracy of quantitative PET measurements.

However, the availability of post-injection transmission method might be limited. This is because post-injection transmission method depends on the assumption that emission distribution between emission and transmission acquisition durations is the same. If emission distribution in each internal organ were changing over time between emission and transmission acquisition durations, attenuation coefficient map could be inaccurate due to the mismatch between extra emission counts and previous emission data. In our phantom study, ^{18}F distribution in a chest phantom was considered to be stable between emission and transmission scan. Thus, extra emission counts were not over or undersubstracted at any region of LV myocardium of a cardiac phantom. In the clinical setting, ^{18}F-FDG PET study is performed when the distribution of ^{18}F-FDG has reached equilibrium in each internal organ, so that the subtraction of extra emission counts from transmission data would also be performed virtually as accurately as our phantom study. In fact, van der Weert et al.[15] reported when data from the last emission frame were used to correct for emission contamination in post-injection transmission data, values of myocardial ^{18}F-FDG activity in 16 patients were, on average, 6% lower than with post-injection transmission method, and no significant differences in the mean normalized ^{18}F-FDG uptake were observed between pre- and post-injection transmission methods, even in segments with decreased ^{18}F-FDG activity. Additionally, in our clinical study, measured defect sizes by post-injection transmission method showed a good correlation with those by pre-injection transmission method. This result indicates that the distribution of ^{13}N-ammonia would not significantly change between emission and transmission scans. Thus, post-injection transmission method can also be applied to ^{13}N-ammonia study for measurement of myocardial defect size. The accuracy of post-injection transmission method is related to other factors, such as the activity of transmission source, transmission and emission acquisition time.[9] Although those factors were not investigated in this study, we considered that they were reliable enough to achieve the accuracy of quantitative PET measurements.

Quantitative PET measurements require a perfect match between emission and transmission data for attenuation correction. The misalignment between emission and transmission data would interface with the accurate attenuation correction, resulting in the failure of estimating

defect size.[6,14] Patients were kept on the scanner bed for a long duration. Thus, patient translation might occur in some cases. Although this study cannot address this issue, we suggest that the effect of patient translation on a scanner bed should be smaller in post-injection transmission method, because of the shorter duration study of the study, than in pre-injection transmission method.

Thus, post-injection transmission method can provide information on defect size, similar to pre-injection transmission method and improve patient comfort and throughput much more than pre-injection transmission method.

CONCLUSION

The results indicate that cardiac PET imaging with post-injection transmission scan provides information on myocardial tracer activity as well as myocardial defect size comparable to conventional pre-injection transmission method. Thus, the post-injection transmission method may serve as an accurate alternative to conventional pre-injection transmission scan technique especially when patients are unable to lie on the scanner bed for a long period.

REFERENCES

1. Tillisch J, Brunken R, Marshall R, Schwaiger M, Mandelkern M, Phelps M. Reversibility of cardiac wall-motion abnormalities predicted by positron tomography. *N Engl J Med* 1986; 314: 884–888.
2. vom Dahl J, Eitzman DT, al-Aouar ZR, Kanter HL, Hicks RJ, Deeb GM. Relation of regional function, perfusion, and metabolism in patients with advanced coronary artery disease undergoing surgical revascularization. *Circulation* 1994; 90: 2356–2366.
3. Tamaki N, Kawamoto M, Tadamura E, Magata Y, Yonekura Y, Nohara R. Prediction of reversible ischemia after revascularization. Perfusion and metabolic studies with positron emission tomography. *Circulation* 1995; 91: 1697–1705.
4. Huang SC, Hoffman EJ, Phelps ME, Kuhl DE. Quantitation in positron emission computed tomography: 2. Effects of inaccurate attenuation correction. *J Comput Assist Tomogr* 1979; 3: 804–814.
5. Hooper PK, Meikle SR, Eberl S, Fulham MJ. Validation of postinjection transmission measurements for attenuation correction in neurological FDG-PET studies. *J Nucl Med* 1996; 37: 128–136.
6. Bettinardi V, Gilardi MC, Lucignani G, Landoni C, Rizzo G, Striano G. A procedure for patient repositioning and compensation for misalignment between transmission and emission data in PET heart studies. *J Nucl Med* 1993; 34: 137–142.
7. Matsunari I, Yoneyama T, Kanayama S, Matsudaira M, Nakajima K, Taki J. Phantom studies for estimation of defect size on cardiac (18)F SPECT and PET: implications for myocardial viability assessment. *J Nucl Med* 2001; 42: 1579–1585.
8. DeGrado TR, Turkington TG, Williams JJ, Stearns CW, Hoffman JM, Coleman RE. Performance characteristics of a whole-body PET scanner. *J Nucl Med* 1994; 35: 1398–1406.
9. Carson RE, Daube-Witherspoon ME, Green MV. A method for postinjection PET transmission measurements with a rotating source. *J Nucl Med* 1988; 29: 1558–1567.
10. Turkington TG, Coleman RE. An evaluation of post-injection transmission measurement in PET. *IEEE Trans Nucl Sci* 1994; 41: 1538–1544.
11. Nekolla SG, Miethaner C, Nguyen N, Ziegler SI, Schwaiger M. Reproducibility of polar map generation and assessment of defect severity and extent assessment in myocardial perfusion imaging using positron emission tomography. *Eur J Nucl Med* 1998; 25: 1313–1321.
12. Matsunari I, Boning G, Ziegler SI, Nekolla SG, Stollfuss JC, Kosa I. Attenuation-corrected ^{99m}Tc-tetrofosmin single-photon emission computed tomography in the detection of viable myocardium: comparison with positron emission tomography using ^{18}F-fluorodeoxyglucose. *J Am Coll Cardiol* 1998; 32: 927–935.
13. O'Connor MK, Gibbons RJ, Juni JE, O'Keefe J Jr, Ali A. Quantitative myocardial SPECT for infarct sizing: feasibility of a multicenter trial evaluated using a cardiac phantom. *J Nucl Med* 1995; 36: 1130–1136.
14. Bland JM, Altman DG. Statistical methods for assessing agreement between two methods of clinical measurement. *Lancet* 1986; 1: 307–310.
15. Matsunari I, Boning G, Ziegler SI, Kosa I, Nekolla SG, Ficaro EP. Effects of misalignment between transmission and emission scans on attenuation-corrected cardiac SPECT. *J Nucl Med* 1998; 39: 411–416.
16. van der Weerdt AP, Boellaard R, Knaapen P, Visser CA, Lammertsma AA, Visser FC. Postinjection transmission scanning in myocardial ^{18}F-FDG PET studies using both filtered backprojection and iterative reconstruction. *J Nucl Med* 2004; 45 (2): 169–175.